2024. 20(1). 27–39

СТРОИТЕЛЬНАЯ МЕХАНИКА ИНЖЕНЕРНЫХ КОНСТРУКЦИЙ И СООРУЖЕНИЙ

STRUCTURAL MECHANICS OF ENGINEERING CONSTRUCTIONS AND BUILDINGS

HTTP://JOURNALS.RUDN.RU/STRUCTURAL-MECHANICS

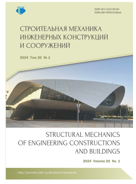

ТЕОРИЯ ПЛАСТИЧНОСТИ
THEORY OF PLASTICITY

DOI: 10.22363/1815-5235-2024-20-1-27-39
UDC 539.3
EDN: XNRJTY

Research article / Научная статья

Mixed FEM for Shells of Revolution Based on Flow Theory and its Modifications

Rumia Z. Kiseleva[1] ✉, **Natalia A. Kirsanova**[2], **Anatoliy P. Nikolaev**[1], **Yuriy V. Klochkov**[1], **Vitaliy V. Ryabukha**[1]

[1] Volgograd State Agrarian University, *Volgograd, Russia*
[2] Financial University under the Government of the Russian Federation, *Moscow, Russia*
✉ rumia1970@yandex.ru

Article history

Received: September 21, 2023
Revised: December 3, 2023
Accepted: December 17, 2023

Conflicts of interest

The authors declare that there is no conflict of interest.

Authors' contribution

Undivided co-authorship.

Abstract. For describing elastoplastic deformation, three versions of constitutive equations are used. The first version employs the governing equations of the flow theory. In the second version, elastic strain increments are defined the same way as in the flow theory, and the plastic strain increments are expressed in terms of stress increments using the condition of their proportionality to the components of the incremental stress deviator tensor. In the third version, the constitutive equations for a load step were obtained without using the hypothesis of separating strains into the elastic and plastic parts. To obtain them, the condition of proportionality of the components of the incremental strain deviator tensor to the components of the incremental stress deviator tensor was applied. The equations are implemented using a hybrid prismatic finite element with a triangular base. A sample calculation shows the advantage of the third version of the constitutive equations.

Keywords: shell of revolution, physical nonlinearity, prismatic finite element, mixed functional, implementation of mixed FEM

For citation

Kiseleva R.Z., Kirsanova N.A., Nikolaev A.P., Klochkov Yu.V., Ryabukha V.V. Mixed FEM for shells of revolution based on flow theory and its modifications. *Structural Mechanics of Engineering Constructions and Buildings.* 2024;20(1):27–39. http://doi.org/10.22363/1815-5235-2024-20-1-27-39

Rumia Z. Kiseleva, Candidate of Technical Sciences, Associate Professor of the Department of Applied Geodesy, Environmental Management and Water Management, Volgograd State Agrarian University, Volgograd, Russia; ORCID: 0000-0002-3047-5256; E-mail: rumia1970@yandex.ru

Natalia A. Kirsanova, Doctor of Physical and Mathematical Sciences, Professor of the Department of Mathematics, Financial University under the Government of the Russian Federation, Moscow, Russia; ORCID: 0000-0003-3496-2008; E-mail: nagureeve@fa.ru

Anatoliy P. Nikolayev, Doctor of Technical Sciences, Professor of the Department of Mechanics, Volgograd State Agrarian University, Volgograd, Russia; ORCID: 0000-0002-7098-5998; E-mail: anpetr40@yandex.ru

Yuriy V. Klochkov, Doctor of Technical Sciences, Professor, Head of the Department of Higher Mathematics, Volgograd State Agrarian University, Volgograd, Russia; ORCID: 0000-0002-1027-1811; E-mail: klotchkov@bk.ru

Vitaliy V. Ryabukha, Postgraduate student of the Department of Mechanics, Volgograd State Agrarian University, Volgograd, Russia; ORCID: 0000-0002-7394-8885; E-mail: vitalik30090@mail.ru

Смешанная формулировка МКЭ в расчете оболочек вращения на основе теории течения и ее модификаций

Р.З. Киселева[1]✉, **Н.А. Кирсанова**[2], **А.П. Николаев**[1], **Ю.В. Клочков**[1], **В.В. Рябуха**[1]

[1] Волгоградский государственный аграрный университет, *Волгоград, Россия*
[2] Финансовый университет при Правительстве Российской Федерации, *Москва, Россия*
✉ rumia1970@yandex.ru

История статьи
Поступила в редакцию: 21 сентября 2023 г.
Доработана: 3 декабря 2023 г.
Принята к публикации: 17 декабря 2023 г.

Заявление о конфликте интересов
Авторы заявляют об отсутствии конфликта интересов.

Вклад авторов
Нераздельное соавторство.

Аннотация. Для учета упругопластического деформирования используются физические уравнения в трех вариантах. В первом варианте применяются определяющие уравнения теории течения, во втором варианте физических уравнений приращения упругих деформаций определяются, как и в теории течения, а приращения пластических деформаций выражаются через приращения напряжений с использованием условия их пропорциональности компонентам девиатора приращений напряжений, в третьем варианте физические уравнения на шаге нагружения получены без гипотезы о разделении деформаций на упругие и пластические части. Для их получения использовано условие пропорциональности компонент девиаторов приращений деформаций компонентам девиаторов приращений напряжений. Реализация уравнений выполнена с использованием гибридного призматического конечного элемента с треугольным основанием, на конкретном примере показано преимущество третьего варианта физических уравнений.

Ключевые слова: оболочка вращения, физическая нелинейность, призматический конечный элемент, смешанный функционал, реализация смешанного МКЭ

Для цитирования
Kiseleva R.Z., Kirsanova N.A., Nikolaev A.P., Klochkov Yu.V., Ryabukha V.V. Mixed FEM for shells of revolution based on flow theory and its modifications // Строительная механика инженерных конструкций и сооружений. 2024. Т. 20. № 1. С. 27–39. http://doi.org/10.22363/1815-5235-2024-20-1-27-39

1. Introduction

For the majority of deformable materials, Hook's law is only valid at loading levels, at which the stresses do not exceed the yield stress of the material. Usually, plastic deformations emerge in stress concentration zones already at insignificant levels of loading. Hence, structural analysis with account of elastoplastic deformation zones is an important engineering problem.

Two elastoplastic deformation theories are most commonly used for solid bodies: flow plasticity theory and the theory of incremental elastoplastic deformation[1] [1–3].

Displacement-based finite element method (FEM) has been widely used for elastoplastic deformation analysis[2] [4–7]. This method was applied to thermoplastic and contact problems of continuum mechanics [8–12].

Киселева Румия Зайдуллаевна, кандидат технических наук, доцент кафедры прикладной геодезии, природообустройства и водопользования, Волгоградский государственный аграрный университет, Волгоград, Россия; ORCID: 0000-0002-3047-5256; E-mail: rumia1970@yandex.ru
Кирсанова Наталья Анатольевна, доктор физико-математических наук, профессор департамента математики, Финансовый университет при Правительстве Российской Федерации, Москва, Россия; ORCID: 0000-0003-3496-2008; E-mail: nagureeve@fa.ru
Николаев Анатолий Петрович, доктор технических наук, профессор кафедры механики, Волгоградский государственный аграрный университет, Волгоград, Россия; ORCID: 0000-0002-7098-5998; E-mail: anpetr40@yandex.ru
Клочков Юрий Васильевич, доктор технических наук, профессор, заведующий кафедрой высшей математики, Волгоградский государственный аграрный университет, Волгоград, Россия; ORCID: 0000-0002-1027-1811; E-mail: klotchkov@bk.ru
Рябуха Виталий Васильевич, аспирант кафедры механики, Волгоградский государственный аграрный университет, Волгоград, Россия; ORCID: 0000-0002-7394-8885; E-mail: vitalik30090@mail.ru

[1] Malinin M.M. *Applied Theory of Plasticity and Creep*. Moscow: Engineering; 1975. (In Russ.); Samul V.I. *Fundamentals of the theory of elasticity and plasticity*: a textbook for university students. 2nd ed., revised. Moscow: Vysshaya shkola Publ.; 1982. (In Russ.); Samul V.I. *Fundamentals of the theory of elasticity and plasticity*: a textbook for university students. 2nd ed., revised. Moscow: Vysshaya shkola Publ.; 1982. (In Russ.)

[2] Levin V.A. *Nonlinear Computational Mechanics of Strength. Models and methods*. Moscow: Fizmatlit. Publ.; 2015. (In Russ.)

FEM was also effectively employed in finite strain cases of elastoplastic deformation processes [13–16]. Mixed finite element method has been extensively applied to elastoplastic deformation problems [17–21].

In this study, a prismatic finite element with triangular bases has been developed in mixed FEM formulation. Three versions of governing equations are used as constitutive relations. The first version uses the flow theory equations. The second version employs the governing equations obtained from the authors' hypothesis, that the components of the incremental plastic strain tensor are proportional to the components of the combined stress deviator tensor.

The third version does not separate strains into the elastic and plastic parts. For determining the relationships between the strain increments and the stress increments, the condition of proportionality between the components of the incremental strain deviator tensor to the components of the incremental stress deviator tensor was used.

2. Methods

2.1. Shell Geometry

Arbitrary point M^{0t} of the shell, which is located at distance t from the middle surface, is defined by the following position vector:

$$\vec{R}^{0t} = \vec{R}^{0} + t\vec{a}^{0}, \tag{1}$$

where $\vec{\mathbf{R}}^{0} = x\vec{\mathbf{i}} + r\sin\theta\,\vec{\mathbf{j}} + r\cos\theta\vec{\mathbf{k}}$ is the position vector of the corresponding point M^0 of the middle surface; r is the radius of curvature of the middle surface point; $\vec{i}, \vec{j}, \vec{k}$ are the unit vectors of the Cartesian coordinate system; x,θ are the axial and angular coordinates of point M^0; $\vec{a}^{0} = \vec{a}_1^{0} \times \vec{a}_1^{0}$ is the normal line to the middle surface at point M^0; $\vec{a}_1^{0} \times \vec{a}_1^{0}$ are the unit basis vectors at point M^0.

The basis vectors of arbitrary point M^{0t} are determined by differentiating position vector (1):

$$\vec{\mathbf{g}}_1^{0} = \vec{\mathbf{R}}^{0t}_{,s}; \quad \vec{\mathbf{g}}_2^{0} = \vec{\mathbf{R}}^{0t}_{,r\theta}; \quad \vec{\mathbf{g}}_3^{0} = \vec{\mathbf{R}}^{0t}_{,t} = \vec{a}^{0}, \tag{2}$$

and by following [17], the matrix expressions of the derivatives of the basis vectors of an arbitrary point in the basis of this point are formed:

$$\underset{3\times1}{\left\{\vec{g}^{0}_{,s}\right\}} = \underset{3\times3}{\left[m\right]}\underset{3\times1}{\left\{\vec{g}^{0}\right\}}; \quad \underset{3\times1}{\left\{\vec{\mathbf{g}}^{0}_{,r\theta}\right\}} = \underset{3\times3}{\left[n\right]}\underset{3\times1}{\left\{\vec{g}^{0}\right\}}; \quad \underset{3\times1}{\left\{\vec{\mathbf{g}}^{0}_{,t}\right\}} = \underset{3\times3}{\left[l\right]}\underset{3\times1}{\left\{\vec{g}^{0}\right\}}, \tag{3}$$

where $\underset{1\times3}{\left\{\vec{g}^{0}_{,s}\right\}^{T}} = \left\{\vec{g}^{0}_{,s1}\ \vec{g}^{0}_{,s2}\ \vec{g}^{0}_{,s3}\right\}$; $\underset{1\times3}{\left\{\vec{g}^{0}_{,r\theta}\right\}^{T}} = \left\{\vec{g}^{0}_{,r_1\theta}\ \vec{g}^{0}_{,r_2\theta}\ \vec{g}^{0}_{,r_3\theta}\right\}$; $\underset{1\times3}{\left\{\vec{g}^{0}_{,t}\right\}^{T}} = \left\{\vec{g}^{0}_{,t1}\ \vec{g}^{0}_{,t2}\ \vec{g}^{0}_{,t3}\right\}$;

$\underset{1\times3}{\left\{\vec{g}^{0}\right\}^{T}} = \left\{\vec{g}_1^{0}\ \vec{g}_2^{0}\vec{g}_3^{0}\right\}$ are the row matrices of the derivatives of the basis vectors of M^{0t}.

Under gradually applied load, the incremental displacement vector at a load step is represented by components in the basis of point M^{0t}:

$$\Delta\vec{V} = \Delta v^{1}\vec{g}_1^{0} + \Delta v^{2}\vec{g}_2^{0} + \Delta v^{3}\vec{g}_3^{0} = \underset{1\times3}{\left\{\vec{g}^{0}\right\}^{T}}\underset{3\times1}{\left\{\Delta v\right\}}, \tag{4}$$

where $\underset{1\times3}{\left\{\Delta v\right\}^{T}} = \left\{\Delta v^{1}\ \Delta v^{2}\ \Delta v^{3}\right\}$ is the row matrix of displacements of point M^{0t}.

The derivatives of the displacement vector are also expressed in terms of the basis vectors of point M^{0t}:

$$\begin{aligned}\Delta\vec{V}_{,s} &= f_1^1\vec{g}_1^0 + f_1^2\vec{g}_2^0 + f_1^3\vec{g}_3^0;\\ \Delta\vec{V}_{,r\theta} &= f_2^1\vec{g}_1^0 + f_2^2\vec{g}_2^0 + f_2^3\vec{g}_3^0;\\ \Delta\vec{V}_{,t} &= f_3^1\vec{g}_1^0 + f_3^2\vec{g}_2^0 + f_3^3\vec{g}_3^0,\end{aligned} \tag{5}$$

where

$f_1^1 = \Delta v_{,s}^1 + \Delta v^1 m_{11} + \Delta v^2 m_{21} + \Delta v^3 m_{31}; \cdots f_3^3 = \Delta v_{,t}^3 + \Delta v^1 l_{13} + \Delta v^2 l_{23} + \Delta v^3 l_{33};$

m_{ij}, n_{ij}, l_{ij} are the elements of matrices $[m]$, $[n]$ and $[l]$.

Under specified load, an arbitrary point of the shell will displace to position M^t, which is determined by position vector

$$\vec{R}^t = \vec{R}^{0t} + \Delta\vec{V}. \tag{6}$$

The strain increments for a load step are governed by relations [3] in a geometrically linear definition

$$\Delta\varepsilon_{ij} = \frac{1}{2}\left(\vec{g}_i^0 \cdot \Delta\vec{v}_{,j} + \vec{g}_j^0 \cdot \Delta\vec{v}_{,i}\right). \tag{7}$$

Considering (5), strains (7) can be expressed in matrix form as

$$\underset{6\times1}{\{\Delta\varepsilon\}} = \underset{6\times3}{[L]}\underset{3\times1}{\{\Delta v\}}, \tag{8}$$

where $\underset{1\times6}{\{\Delta\varepsilon\}^T} = \{\Delta\varepsilon_{ss}\ \Delta\varepsilon_{\theta\theta}\ \Delta\varepsilon_{tt}\ 2\Delta\varepsilon_{s\theta}\ 2\Delta\varepsilon_{st}\ 2\Delta\varepsilon_{\theta t}\}$ is the row matrix of strain increments; $[L]$ is the matrix of differentiation operators.

2.2. Relations of Flow Plasticity Theory

Full strain increments $\Delta\varepsilon_{ij}$ are combinations of elastic strains $\Delta\varepsilon_{ij}^e$ and plastic strains $\Delta\varepsilon_{ij}^p$:

$$\Delta\varepsilon_{ij} = \Delta\varepsilon_{ij}^e + \Delta\varepsilon_{ij}^p. \tag{9}$$

The relationships between the elastic strain increments and the stress increments are defined by expressions[3]

$$\Delta\varepsilon_{ij}^e = \frac{1}{E}\left[(1-\nu)\Delta\sigma_{ij} - \nu\Delta\sigma_c\delta_{ij}\right], \tag{10}$$

where E is the material Young's modulus; ν is the Poisson's ratio; $\Delta\sigma_c$ is the mean value of the normal stress increments; δ_{ij} is the Kronecker delta.

In the flow theory, the plastic strain increments are defined by relations[4]

[3] Samul V.I. *Fundamentals of the theory of elasticity and plasticity*: a textbook for university students. 2nd ed., revised. Moscow: Vysshaya shkola; 1982. (In Russ.); Demidov S.P. Theory of elasticity. Moscow: Vysshaya shkola; 1979. (In Russ.); Demidov S.P. Theory of elasticity. M.: Vysshaya shkola; 1979. (In Russ.)

[4] Malinin M.M. *Applied Theory of Plasticity and Creep*. Moscow: Engineering; 1975. (In Russ.)

$$\Delta\varepsilon_{ij}^{p} = k\left(\sigma_{ij} - \sigma_c \delta_{ij}\right), \tag{11}$$

where k is the coefficient of proportionality, which is defined according to[6] expression

$$k = \frac{3}{2\sigma_i}\left(\frac{1}{E_k} - \frac{1}{E_н}\right)\Delta\sigma_i . \tag{12}$$

Here: σ_i is the stress intensity; $E_н$ is the modulus of the initial segment of the stress-strain intensity diagram; $E_к$ is the tangent modulus at the considered point on the stress-strain intensity diagram; $\Delta\sigma_i = \frac{\partial\sigma_i}{\partial\sigma_{mn}}\Delta\sigma_{mn}$ is the stress intensity increment.

By combining (10) and (11) and taking into account (12), the matrix expression for the constitutive equations of the flow theory is formed:

$$\underset{6\times1}{\left\{\Delta\varepsilon\right\}} = \underset{6\times6}{\left\{C_1^{П}\right\}}\underset{6\times1}{\left\{\Delta\sigma\right\}} . \tag{13}$$

The second version of the post-yield constitutive equations uses the hypothesis of proportionality between the components of the incremental plastic strain tensor and the components of the incremental stress deviator tensor:

$$\Delta\varepsilon_{ij}^{p} = \psi_1\left(\Delta\sigma_{ij} - \Delta\sigma_c \delta_{ij}\right). \tag{14}$$

Proportionality coefficient ψ_1 is defined according to[5] expression

$$\psi_i = \frac{3}{2}\left(\frac{1}{E_k} - \frac{1}{E_н}\right). \tag{15}$$

By combining (10) and (14), the matrix expression for the second version of constitutive relations is obtained:

$$\underset{6\times1}{\left\{\Delta\varepsilon\right\}} = \underset{6\times6}{\left[C_2^{П}\right]}\underset{6\times1}{\left\{\Delta\sigma\right\}} . \tag{16}$$

The third version of constitutive relations is based on the hypothesis of proportionality between the incremental strain deviator tensor and the incremental stress deviator tensor components:

$$\Delta\varepsilon_{ij} - \delta_{ij}\Delta\varepsilon_c = \psi_2(\Delta\sigma_{ij} - \delta_{ij}\Delta\sigma_c), \tag{17}$$

where $\psi_2 = \frac{3}{2}\frac{\Delta\varepsilon_i}{\Delta\sigma_i} = \frac{3}{2}\frac{1}{E_k}$, and the volumetric strain increment is determined as in the case of elastic deformation, $\Delta\varepsilon_c = \Delta\sigma_c \frac{1-2\nu}{E}$.

Based on (17), the third version of the constitutive relations is formed:

$$\left\{\Delta\varepsilon\right\} = \left[C_3^{П}\right]\left\{\Delta\sigma\right\} . \tag{18}$$

[5] Malinin M.M. *Applied Theory of Plasticity and Creep*. Moscow: Engineering; 1975. (In Russ.)

2.3. Finite Element Stiffness Matrix

A prismatic finite element with triangular bases is considered. The nodal unknowns are the displacement and stress increments. Coordinates s, θ, t of an arbitrary point of the shell are defined in terms of nodal coordinates using linear functions ξ, η, ζ with ranges $0 \le \xi, \eta \le 1$; $-1 \le \zeta \le 1$,

$$\lambda = \underset{1\times6}{\{f(\xi,\eta,\zeta)\}^T} \underset{6\times1}{\{\lambda_y\}}, \tag{19}$$

where $\{\lambda_y\}^T = \{\lambda^i \; \lambda^j \; \lambda^k \; \lambda^m \; \lambda^n \; \lambda^p\}$ is the row of nodal coordinate s, θ or t;

$$\underset{1\times6}{\{f(\xi,\eta,\zeta)\}^T} = \left\{(1-\xi-\eta)\frac{1-\zeta}{2} \vdots \xi\frac{1-\zeta}{2} \vdots \eta\frac{1-\zeta}{2} \vdots (1-\xi-\eta)\frac{1+\zeta}{2} \vdots \xi\frac{1+\zeta}{2} \vdots \eta\frac{1+\zeta}{2}\right\}$$

By using linear approximating functions (19), the interpolation expressions for Δv components and the components of the incremental stress tensor are formed:

$$\underset{3\times1}{\{\Delta v\}} = \underset{3\times18}{[A]} \underset{18\times1}{\{\Delta v_y\}}, \quad \underset{6\times1}{\{\Delta\sigma\}} = \underset{6\times36}{[S]} \underset{36\times1}{\{\Delta\sigma_y\}}, \tag{20}$$

where $\underset{1\times18}{\{\Delta v_y\}^T} = \{\Delta v^{1i} \; \Delta v^{1j} \Delta v^{1k} \Delta v^{2i} \Delta v^{2j} \Delta v^{2k} \ldots \; \Delta v^{3m} \Delta v^{3n} \Delta v^{3p}\}$ is the row-matrix of the nodal displacement increments;

$\underset{1\times6}{\{\Delta\sigma\}^T} = \{\Delta\sigma_{ss} \Delta\sigma_{\theta\theta} \Delta\sigma_{tt} \Delta\sigma_{s\theta} \Delta\sigma_{st} \Delta\sigma_{\theta t}\}$ is the row of stress increments at a point;

$\underset{1\times36}{\{\Delta\sigma_y\}^T} = \left\{\underset{1\times6}{\{\Delta\sigma_{ssy}\}^T} \underset{1\times6}{\{\Delta\sigma_{\theta\theta y}\}^T} \cdots \underset{1\times6}{\{\Delta\sigma_{\theta ty}\}^T}\right\}$ is the row of stress increments at the nodes of the finite element.

Considering (20), strain increments (8) can be represented in matrix form:

$$\underset{6\times1}{\{\Delta\varepsilon\}} = \underset{6\times3}{[L]} \underset{3\times1}{\{\Delta v\}} = \underset{6\times3}{[L]} \underset{3\times18}{[A]} \underset{18\times1}{\{\Delta v_y\}} = \underset{6\times18}{[B]} \underset{18\times1}{\{\Delta v_y\}}. \tag{21}$$

The nonlinear mixed functional for a load step, obtained in [17], is expressed as

$$\Phi \equiv \int_V \underset{1\times6}{\{\Delta\sigma\}^T} \underset{6\times3}{[L]} \underset{3\times1}{\{\Delta v\}} dV - \frac{1}{2}\int_V \underset{1\times6}{\{\Delta\sigma\}^T} \underset{6\times6}{\left[C_\mu^{\Pi}\right]} \underset{3\times1}{\{\Delta\sigma\}} dV -$$

$$-\frac{1}{2}\int_S \underset{1\times3}{\{\Delta v\}^T} \underset{3\times1}{\{\Delta q\}} dS - \int_S \underset{1\times3}{\{\Delta v\}^T} \underset{3\times1}{\{q\}} dS + \int_V \underset{1\times6}{\{\sigma\}^T} \underset{6\times1}{\{\Delta\varepsilon\}} dV; \quad (\mu = 1,2,3). \tag{22}$$

Taking into account matrix relations (18) and (21), functional (22) for the prismatic finite element becomes

$$\Phi \equiv \underset{1\times36}{\{\Delta\sigma_y\}^T} \int_V \underset{36\times6}{[S]^T} \underset{6\times18}{[B]} dV \underset{18\times1}{\{\Delta v_y\}} - \frac{1}{2} \underset{1\times36}{\{\Delta\sigma_y\}^T} \int_V \underset{36\times6}{[S]^T} \underset{6\times6}{[C^{\Pi}_{\mu}]} \underset{6\times36}{[S]} dV \underset{36\times1}{\{\Delta\sigma_y\}} -$$

$$-\frac{1}{2} \underset{1\times18}{\{\Delta v_y\}^T} \int_S \underset{18\times3}{[A]^T} \underset{3\times1}{\{\Delta q\}} dS - \underset{1\times18}{\{\Delta v_y\}^T} \int_S \underset{18\times1}{[A]^T} \underset{3\times1}{\{q\}} dS + \underset{1\times18}{\{\Delta v_y\}^T} \int_V \underset{18\times6}{[B]^T} \underset{6\times1}{\{\sigma\}} dV. \tag{23}$$

By varying functional (23) with respect to nodal unknowns $\underset{1\times36}{\{\Delta\sigma_y\}^T}$ and $\underset{1\times18}{\{\Delta v_y\}^T}$, the following systems of equations are obtained:

$$\frac{\partial\Phi}{\partial\{\Delta\sigma_y\}^T} \equiv \underset{36\times18}{[Q]} \underset{18\times1}{\{\Delta v_y\}} - \underset{36\times36}{[H]} \underset{36\times1}{\{\Delta\sigma_y\}} = 0; \quad \frac{\partial\Phi}{\partial\{\Delta v_y\}^T} \equiv \underset{18\times36}{[Q]^T} \underset{36\times1}{\{\Delta\sigma\}} - \underset{18\times1}{\{\Delta f_q\}} - \underset{18\times1}{\{R\}} = 0, \tag{24}$$

where $\underset{36\times18}{[Q]} = \int_V \underset{36\times6}{[S]^T} \underset{6\times18}{[B]} dV$; $\underset{36\times36}{[H]} = \int_V \underset{36\times6}{[S]^T} \underset{6\times6}{[C^{\Pi}_{\mu}]} \underset{6\times36}{[S]} dV$; $\underset{18\times1}{\{\Delta f_q\}} = \int_S \underset{18\times3}{[A]^T} \underset{3\times1}{\{\Delta q\}} dS$;

$\underset{18\times1}{\{R\}} = \int_S \underset{18\times3}{[A]^T} \underset{3\times1}{\{q\}} dS - \int_V \underset{18\times6}{[B]^T} \underset{6\times1}{\{\sigma\}} dV$ is the Raphson residual.

Systems (24) can be combined into one

$$\underset{54\times54}{[K]} \underset{54\times1}{\{Z_y\}} = \underset{54\times1}{\{F_y\}}, \tag{25}$$

where $\underset{54\times54}{[K]} = \begin{bmatrix} -\underset{36\times36}{[H]} & \underset{36\times18}{[Q]} \\ \underset{18\times36}{[Q]^T} & \underset{18\times18}{[0]} \end{bmatrix}$ — is the matrix of the stress-strain state of the hybrid finite element at a load step; $\underset{1\times54}{\{Z_y\}^T} = \left\{ \underset{1\times36}{\{\Delta\sigma_y\}^T} \; \underset{1\times18}{\{\Delta v_y\}^T} \right\}$ — is the vector of nodal unknowns; $\underset{1\times54}{\{F_y\}^T} = \left\{ \underset{1\times36}{\{0\}^T} \vdots \underset{1\times18}{\{\Delta f_q\}^T} + \underset{1\times18}{\{R\}^T} \right\}$ — is the vector of nodal loads with residuals.

3.1. Sample Calculation 1

The shell of revolution depicted in Figure 1 with the middle surface in the shape of a truncated ellipsoid was analyzed. The following input values were specified: $a = 0.21$ m; $в = 0.15$ m; $h = 0.01$ m; $l_k = 0.2$ m; $E = 2\times10^5$ MPa; $\nu = 0.3$. The height of truncation of the elliptical shell is

$$z_k = в \cdot \sqrt{1 - \frac{l_k^{\,2}}{a^2}} = 0.15 \cdot \sqrt{1 - \frac{0.20^2}{0.21^2}} = 0.0457 \text{ m.}$$

The stress-strain curve for the shell material was assumed to be in the form of Figure 2, where $\sigma_T = 200$ MPa is the yield stress of the material; $\varepsilon_T = 0.001$ is the yield strain; $\varepsilon_k = 0.02$ is the final strain; $\sigma_k = 400$ MPa is the final stress.

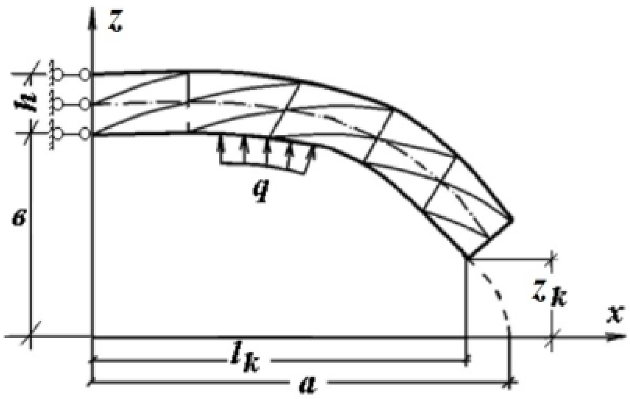

Figure 1. Truncated elliptical shell
Source: made by R.Z. Kiseleva

The stress-strain intensity curve was constructed using formulas[6]

$$\sigma_i = \frac{1}{\sqrt{2}}\left[\left(\sigma_{11}-\sigma_{22}\right)^2+\left(\sigma_{22}-\sigma_{33}\right)^2+\left(\sigma_{33}-\sigma_{11}\right)^2\right] = \frac{1}{\sqrt{2}}\left[\sigma^2+0+\sigma^2\right]=\sigma;$$

$$\varepsilon_i = \frac{\sqrt{2}}{3}\left[\left(\varepsilon_{11}-\varepsilon_{22}\right)^2+\left(\varepsilon_{22}-\varepsilon_{33}\right)^2+\left(\varepsilon_{33}-\varepsilon_{11}\right)^2\right]=\frac{\sqrt{2}}{3}\left[\left(\varepsilon+\nu\varepsilon\right)^2+0+\left(-\nu\varepsilon-\varepsilon\right)^2\right]=\frac{2\left(1+\nu\right)}{3}\varepsilon.$$

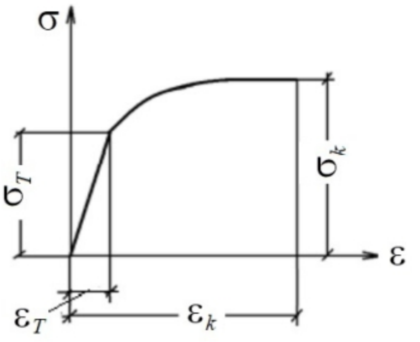

Figure 2. Stress-strain curve of the elliptical shell material
Source: made by R.Z. Kiseleva

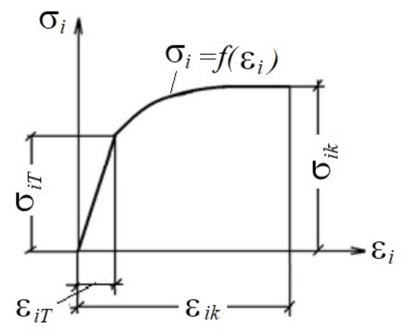

Figure 3. Stress-strain intensity curve of the shell material
Source: made by R.Z. Kiseleva

Values of the parameters of the stress-strain intensity curve: $\sigma_{iT} = \sigma_T = 200$ MPa is the stress intensity at yield point;

$\varepsilon_{iT} = \frac{2}{3}\left(1+\nu\right)\varepsilon_T = \frac{2}{3}\left(1+0.3\right)\cdot 0.001 = 0.866667\times10^{-3}$ is the strain intensity at yield point;

$\varepsilon_{ik} = \frac{2}{3}\left(1+\nu\right)\varepsilon_k = \frac{2}{3}\left(1+0.3\right)\cdot 0.01 = 0.866667\times10^{-2}$ is the final strain intensity;

$\sigma_{i\kappa} = \sigma_\kappa = 300$ MPa is the final stress intensity.

[6] Malinin M.M. Applied Theory of Plasticity and Creep. Moscow: Engineering; 1975. (In Russ.)

The stress-strain intensity curve is assumed to be defined by function $\sigma_i = f(\varepsilon_i)$ in the form of a parabola

$\sigma_i = a\varepsilon_i^2 + b\varepsilon_i + c$ (when $\varepsilon_i > \varepsilon_{iT}$),

where $a = -6612835.5282$ MPa; $b = 242231.47902$ MPa; $c = 1795.0330258$ MPa.

The presented shell of revolution was analyzed for the case of elastic deformation ($q = 18.0$ MPa). The normal stress values at the fixed support are presented in Table 1, where the first column contains the number of discretization nodes of the shell along its axis (*NM*) and along its thickness (*NT*).

The other columns contain normal stresses of the internal fibers along the axis $\left(\sigma_{11}^{\text{int}}\right)$ and circumference $\left(\sigma_{\theta\theta}^{\text{int}}\right)$. For the external fibers, these variables are denotes as $\left(\sigma_{11}^{\text{ext}}\right)$ and $\left(\sigma_{\theta\theta}^{\text{ext}}\right)$ respectively.

Table 1

Numerical values of normal stresses at the fixed support

NM* × *NT	σ_{11}^{int}, **MPa**	$\sigma_{\theta\theta}^{\text{int}}$, **MPa**	σ_{11}^{ext}, **MPa**	$\sigma_{\theta\theta}^{\text{ext}}$, **MPa**
20×3	116.484	210.103	117.640	203.671
40×5	116.324	209.843	118.267	203.857
30×7	116.234	209.766	118.396	203.834

The results presented in Table 1 demonstrate convergence of the computational process with respect to normal stresses of the shell at the fixed support.

3.2. Sample Calculation 2

The analysis of the shell from the previous section was performed under internal pressure $q = 27.65$ MPa. The specified load value was achieved in 16 steps and in 32 steps, and the results of the analysis using the three versions of constitutive equations were found to be virtually identical.

The values of meridional stresses σ_{ss} and circumferential stresses $\sigma_{\theta\theta}$ after 32 load steps are presented in Table 2. The stress values were calculated along the shell thickness *h* in the left section using the third version of the constitutive equations.

Table 2

Numerical values of meridional and circumferential stresses after 32 load steps along the shell thickness *h* in the left section

σ_{ss}, **MPa**	163.8	170.7	175.4	181.8	186.9	193.2	205.4
$\sigma_{\theta\theta}$, **MPa**	323.2	318.9	314.4	313.1	309.0	306.9	302.8
***h*, m**	0	0.00166	0.0033	0.005	0.0066	0.00833	0.01

The of results from Table 2 are used to plot the distributions of meridional stresses (Figure 4) and circumferential stresses (Figure 5).

In order to control the accuracy of computation of meridional stresses, the check of $\sum x = 0$ is performed. The check gives an acceptable discrepancy in the values of the resultant external and internal forces:

$$\delta = \frac{Q_{\text{ext-}Q_{\text{int}}}}{Q_{\text{ext}}} \times 100\% = 2.4\%,$$

where Q_{ext} is the resultant external force; Q_{int} is the resultant internal force.

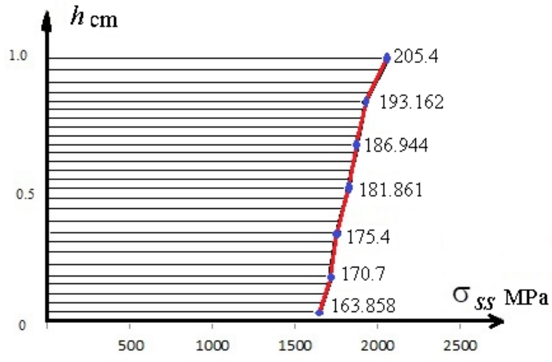

Figure 4. Distribution of meridional stresses σ_{ss} along the section thickness
Source: made by R.Z. Kiseleva

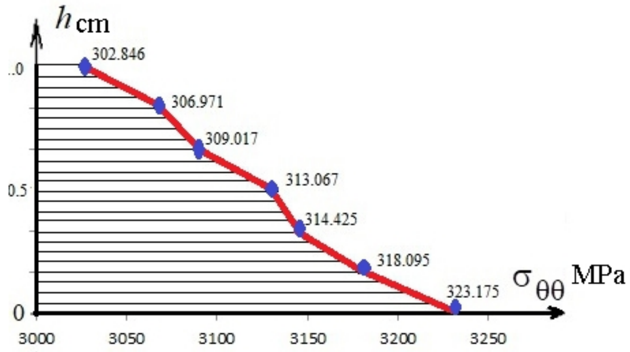

Figure 5. Distribution of circumferential stresses $\sigma_{\theta\theta}$
Source: made by R.Z. Kiseleva

As seen from Figure 5, the circumferential stresses exceed the elastic limit significantly.

Table 3 provides the values of meridional and circumferential stresses in the external fibers along the meridian arc length.

Table 3

Numerical values of meridional and circumferential stresses in external fibers along the meridian arc length

Stress	Meridian arc length *S*, m											
	0.005	0.025	0.04	0.06	0.081	0.102	0.124	0.147	0.172	0.185	0.2	0.237
σ_{ss}, MPa	164.2	165.0	164.6	163.1	161.0	157.1	152.9	150.0	142.2	134.9	121.0	0.6
$\sigma_{\theta\theta}$, MPa	302.9	302.7	301.0	295.6	288.6	279.5	267.7	254.5	249.5	242.7	244.0	251.1

The results from Table 3 were used to plot the distributions of meridional stresses σ_{ss} and circumferential stresses $\sigma_{\theta\theta}$ (Figure 6).

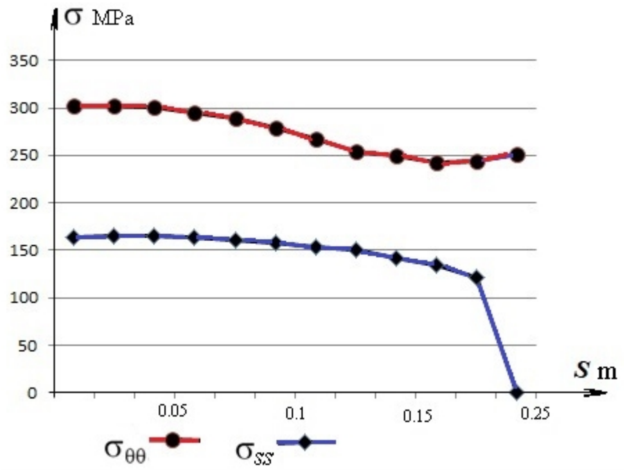

Figure 6. Distributions of meridional and circumferential stresses in external fibers along the meridian arc length
Source: made by R.Z. Kiseleva

The values of the meridional stresses in the end section are almost zero, which complies with the loading condition. The circumferential stresses vary insignificantly along the meridian.

The analysis of the results in Tables 1–3 indicates correctness of the developed algorithm and shows adequate convergence of the computational process.

4. Conclusion

The 3D stress-strain state of a shell is studied without using the straight-normal hypothesis for elastoplastic deformation.

1. *The constitutive relations beyond the elastic limit are implemented in three versions.*

The first version uses the relationships of the flow theory.

The second version employs the governing equations, where the authors' hypothesis is used for determining the plastic strain increments. The hypothesis assumes that the components of the incremental plastic strain tensor are proportional to the components of the incremental stress deviator tensor.

The third version of equations is based on the hypothesis of proportionality between the components of the incremental strain deviator tensor and the components of the incremental stress deviator tensor without separating the strains into elastic and plastic.

2. *The analysis of the shell is performed using mixed FEM.* For this purpose, the authors developed a 6-node solid prismatic finite element with triangular bases. The nodal unknowns are the displacement vector components and the nodal stress tensor components. The target variables are approximated by the nodal unknowns using bilinear shape functions.

3. *The presented study shows that all three versions of the governing equations for plastic deformation produce identical results.* The analysis of the constitutive equations shows that the most physically reasonable version is the third one. This version does not separate the strain increments into elastic and plastic parts, and is based on the hypothesis of proportionality between the components of the incremental strain deviator tensor to the components of the incremental stress deviator tensor.

The proposed governing equations, without the strain separation, correspond to the physical meaning of the process of deformation and have great potential for analyzing reservoirs, submersibles and other engineering structures containing shells of revolution.

References

1. Golovanov A.I., Sultanov L.U. *Mathematical Models of Computational Nonlinear Mechanics of Deformable Media*. Kazan: Kazan State un-t; 2009. (In Russ.) EDN: QJWGNN

2. Petrov V.V. *Nonlinear Incremental Structural Mechanics*. Moscow: Infra–Inzheneriya Publ.; 2014. (In Russ.)

3. Sedov L.I. *Continuum Mechanics*. Moscow: Nauka Publ.; 1976; Vol.1. (In Russ.)

4. Bate KYu. *Finite element method: textbook*. Moscow: Fizmatlit Publ.; 2010. (In Russ.)

5. Golovanov A.I., Tyuleneva O.N., Shigabutdinov A.F. *Finite element method in statics and dynamics of thin-walled structures*. Moscow: Fizmatlit Publ.; 2006. (In Russ.) EDN: QJPXPV

6. Krivoshapko S.N., Christian A.B.H., Gil-oulbé M. Stages and architectural styles in design and building of shells and shell structures. *Building and Reconstruction*. 2022;4(102):112–131. https://doi.org/10.33979/2073-7416-2022-102-4-112-131

7. Beirao Da Veiga L., Lovadina C., Mora D. A virtual element method for elastic and inelastic problems on polytope meshes. *Computer Methods in Applied Mechanics and Engineering*. 2017;295:327–346. https://doi.org/10.1016/j.cma.2015.07.013

8. Aldakheev F., Miehe C. Coupled thermomechanical response of gradient plasticity. *International Journal of Plasticity.* 2017;91:1–24. https://doi.org/10.1016/j.ijplas.2017.02.007

9. Aldakheel F. Micromorphic approach for gradient-extended thermo-elastic-plastic solids in the algorithmic strain space. *Continuum Mechanics Thermodynamics.* 2017;29(6):1207–1217. https://doi.org/10.1007/s00161-017-0571-0

10. Sultanov L.U. Computational algorithm for investigation large elastoplastic deformations with contact interaction. *Lobachevskii Journal of Mathematics.* 2021;42(8):2056–2063. https://doi.org/10.1134/S199508022108031X

11. Tupyshkin N.D., Zapara M.A. Defining relations of the tensor theory of plastic damage to metals. *Problems of strength, plasticity and stability in the mechanics of a deformable solid.* Tver: Izd-vo TvGTU; 2011. p. 216–219. (In Russ.)

12. Ilyushin A.A. *Ilyushin A.A. Plasticity. Elastic-plastic deformations*. S-Peterburg: Lenand; 2018.

13. Hanslo P., Larson Mats G., Larson F. Tangential differential calculus and the finite element modeling of a large deformation elastic membrane problem. *Computational Mechanics*. 2015;56(1):87–95.

14. Aldakheei F., Wriggers P. and Miehe C. A modified Gurson-type plasticity model at finite strains: formulation, numerical analysis and phase-field coupling. *Computational Mechanics.* 2018;62:815–833. https://doi.org/10.1007/s00466-017-1530-0

15. Golovanov A.I. Modeling of the large elastoplastic deformations of shells. theoretical basis of finite-element models. *Problems of Strength and Plasticity.* 2010;72:5–17. (In Russ.) EDN: NCVHZV

16. Wriggers P., Hudobivnik B. A low order virtual element formulation for finite elastoplastic deformations. *Computer Methods in Applied Mechanics and Engineering.* 2017;2:123–134. http://doi.org/10.1016/j.cma.:08.053,2017

17. Gureyeva N.A., Arkov D.P. Implementation of the deformation theory of plasticity in calculations of plane-stressed plates based on FEM in a mixed formulation. *Bulletin of higher educational institutions. North caucasus region. Natural sciences*. 2011;2:12–15. (In Russ.) EDN: NUPEON

18. Gureeva N.A., Kiseleva R.Z., Nikolaev A.P. Nonlinear deformation of a solid body on the basis of flow theory and realization of fem in mixed formulation. *IOP Conference Series: Materials Science and Engineering. International Scientific and Practical Conference Engineering*. 2019;675:012059. https://doi.org/10.1088/1757-899X/675/1/012059

19. Gureeva N.A., Klochkov Yu.V., Nikolaev A.P., Yushkin V.N. Stress-strain state of shell of revolution analysis by using various formulations of three-dimensional finite elements. *Structural Mechanics of Engineering Constructions and Buildings.* 2020;16(5):361–379. https://doi.org/10.22363/1815-5235-2020-16-5-361-379

20. Magisano D., Leonetti L., Garcea G. Advantages of mixed format in geometrically nonlinear of beams and shells using solid finite elements. *International Journal for Numerikal Methods Engineering*. 2017:109(9):1237–1262. http://doi.org/10.1002/nme.5322

21. Magisano D., Leonetti L., Garcea G. Koiter asymptotic analysis of multilayered composite structures using mixed solid-shell finite elements. *Composite Structures.* 2016;154:296–308. http://doi.org/10.1016/j.compstruct.2016.07.046

Список литературы

1. *Голованов А.И., Султанов Л.У.* Математические модели вычислительной нелинейной механики деформируемых сред. Казань: Казанский гос. ун-т, 2009. 463 с. EDN: QJWGNN

2. *Петров В.В.* Нелинейная инкрементальная строительная механика. М.: Инфра — Инженерия, 2014. 480 с. EDN: SFTTJV

3. *Седов Л.И.* Механика сплошной среды. М.: Наука, 1976. Т. 1. 536 с.

4. *Бате К.-Ю.* Методы конечных элементов. М.: Физматлит, 2010. 1022 с.

5. *Голованов А.И., Тюленева О.Н., Шигабутдинов А.Ф.* Метод конечных элементов в статике и динамике тонкостенных конструкций. М.: Физматлит, 2006. 391 с. EDN: QJPXPV

6. *Krivoshapko S.N., Christian A.B.H., Gil-oulbé M.* Stages and architectural styles in design and building of shells and shell structures // Строительство и реконструкция. 2022. № 4 (102). С. 112–131. https://doi.org/10.33979/2073-7416-2022-102-4-112-131

7. *Beirao Da Veiga L., Lovadina C., Mora D.* A virtual element method for elastic and inelastic problems on polytope meshes // Computer Methods in Applied Mechanics and Engineering. 2017. Vol. 295. P. 327–346. https://doi.org/10.1016/j.cma.2015.07.013

8. *Aldakheev F., Miehe C.* Coupled thermomechanical response of gradient plasticity // International Journal of Plasticity. 2017. Vol. 91. P. 1–24. https://doi.org/10.1016/j.ijplas.2017.02.007

9. *Aldakheel F.* Micromorphic approach for gradient-extended thermo-elastic-plastic solids in the algorithmic strain space // Continuum Mechanics Thermodynamics. 2017. Vol. 29(6). P. 1207–1217.

10. *Sultanov L.U.* Computational algorithm for investigation large elastoplastic deformations with contact interaction // Lobachevskii Journal of Mathematics. 2021. Vol. 42. No. 8. P. 2056–2063. https://doi.org/10.1134/S199508022108031X

11. *Тутышкин Н.Д., Запара М.А.* Определяющие соотношения тензорной теории пластической повреждаемости металлов // Проблемы прочности, пластичности и устойчивости в механике деформируемого твердого тела. Тверь: Изд-во ТвГТУ, 2011. С. 216–219.

12. *Ilyushin A.A.* Plastichnost. Uprugo-plasticheskiye deformatsii. S-Peterburg: Lenand, 2018. 352 p.

13. *Hanslo P., Larson Mats G., Larson F.* Tangential differential calculus and the finite element modeling of a large deformation elastic membrane problem // Computational Mechanics. 2015. Vol. 56. No. 1. P. 87–95. https://doi.org/10.1007/s00466-015-1158-x

14. *Aldakheei F., Wriggers P., Miehe C.* A modified Gurson-type plasticity model at finite strains: formulation, numerical analysis and phase-field coupling // Computational Mechanics. 2018. Vol. 62. P. 815–833. https://doi.org/10.1007/s00466-017-1530-0

15. *Голованов А.И.* Моделирование больших упругопластических деформаций оболочек. теоретические основы конечно-элементных моделей // Проблемы прочности и пластичности. 2010. № 72. С. 5–17. EDN: NCVHZV

16. *Wriggers P., Hudobivnik B.* A low order virtual element formulation for finite elastoplastic deformations // Computer Methods in Applied Mechanics and Engineering. 2017. Vol. 2. P. 123–134: https://doi.org/10.1016/j.cma.:08.053,2017

17. *Гуреева Н.А., Арьков Д.П.* Реализация деформационной теории пластичности в расчетах плосконапряженных пластин на основе МКЭ в смешанной формулировке // Известия высших учебных заведений. Северо-Кавказский регион. Серия: Естественные науки. 2011. № 2. С. 12–15. EDN: NUPEON

18. *Gureeva N.A., Kiseleva R.Z., Nikolaev A.P.* Nonlinear deformation of a solid body on the basis of flow theory and realization of fem in mixed formulation // IOP Conference Series: Materials Science and Engineering. International Scientific and Practical Conference Engineering. 2019. Vol. 675. Article No. 012059. https://doi.org/10.1088/1757-899X/675/1/012059

19. *Гуреева Н.А., Клочков Ю.В., Николаев А.П., Юшкин В.Н.* Напряженно-деформированное состояние оболочки вращения при использовании различных формулировок трехмерных конечных элементов // Строительная механика инженерных конструкций и сооружений. 2020. Т. 16. № 5. С 361–379. http://doi.org/10.22363/1815-5235-2020-16-5-361-379

20. *Magisano D., Leonetti L., Garcea G.* Advantages of mixed format in geometrically nonlinear of beams and shells using solid finite elements // International Journal for Numerikal Methods Engineering. 2017. Vol. 109. Issue 9. P. 1237–1262. https://doi.org/10.1002/nme.5322

21. *Magisano D., Leonetti L., Garcea G.* Koiter asymptotic analysis of multilayered composite structures using mixed solid-shell finite elements // Composite Struct. 2016. Vol. 154. P. 296–308. https://doi.org/10.1016/j.compstruct.2016.07.046